

# Rapamycin Inhibits Osteoclastogenesis and Prevents LPS-Induced Alveolar Bone Loss by Oxidative Stress Suppression

Chong Feng, Yan Liu, Bao-Yi Zhang, Hao Zhang, Fa-Yu Shan, Tian-Qi Li, Zhi-Ning Zhao, Xin-Xing Wang,\* and Xiang-Yu Zhang\*



Cite This: *ACS Omega* 2023, 8, 20739–20754



Read Online

ACCESS |



Metrics & More

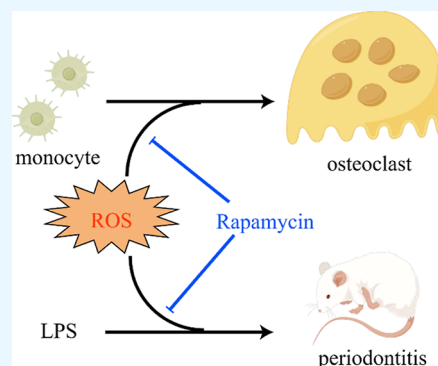


Article Recommendations



Supporting Information

**ABSTRACT:** Periodontitis is a progressive inflammatory skeletal disease characterized by periodontal tissue destruction, alveolar bone resorption, and tooth loss. Chronic inflammatory response and excessive osteoclastogenesis play essential roles in periodontitis progression. Unfortunately, the pathogenesis that contributes to periodontitis remains unclear. As a specific inhibitor of the mTOR (mammalian/mechanistic target of rapamycin) signaling pathway and the most common autophagy activator, rapamycin plays a vital role in regulating various cellular processes. The present study investigated the effects of rapamycin on osteoclast (OC) formation *in vitro* and its effects on the rat periodontitis model. The results showed that rapamycin inhibited OC formation in a dose-dependent manner by up-regulating the Nrf2/GCLC signaling pathway, thus suppressing the intracellular redox status, as measured by 2',7'-dichlorofluorescein diacetate and MitoSOX. In addition, rather than simply increasing the autophagosome formation, rapamycin increased the autophagy flux during OC formation. Importantly, the anti-oxidative effect of rapamycin was regulated by an increase in autophagy flux, which could be attenuated by blocking autophagy with bafilomycin A1. In line with the *in vitro* results, rapamycin treatment attenuated alveolar bone resorption in rats with lipopolysaccharide-induced periodontitis in a dose-dependent manner, as assessed by micro-computed tomography, hematoxylin–eosin staining, and tartrate-resistant acid phosphatase staining. Besides, high-dose rapamycin treatment could reduce the serum levels of proinflammatory factors and oxidative stress in periodontitis rats. In conclusion, this study expanded our understanding of rapamycin's role in OC formation and protection from inflammatory bone diseases.



## INTRODUCTION

Bone tissues undergo continuous remodeling throughout life through a dynamic balance between osteogenesis and osteoclastogenesis, to ensure homeostasis and adaptation to various stresses.<sup>1</sup> Osteoclasts (OCs) are terminally differentiated multinucleated giant cells involved in the matrix resorption of hard tissues and play an important role in bone remodeling.<sup>2</sup> Disruption of the bone remodeling process can result in abnormal bone structure and function, thereby leading to a variety of skeletal disorders.<sup>3</sup> Several inflammatory musculoskeletal disorders in adults, such as periodontitis, rheumatoid arthritis, osteoarthritis, and peri-implantitis, are associated with the loss of bone mass due to excessive OC activity.<sup>4,5</sup> Numerous studies have adopted the strategy of OC differentiation inhibition to alleviate these pathological disorders.

OCs originate from monocyte/macrophage precursor cells from the hematopoietic system and perform the bone resorption function near the surface of the bone/lesion. Their differentiation occurs under the stimulus of two essential cytokines: the receptor activator of nuclear factor  $\kappa$ B ligand (RANKL) and macrophage colony-stimulating factor (M-CSF).<sup>6</sup> The binding of RANKL and the receptor activator of

nuclear factor kappa-B (RANK) initiates a signaling cascade, leading to the transcriptional activation of OC-specific genes.<sup>7</sup> While M-CSF alone cannot induce OC differentiation, it coordinates with RANKL to ensure the survival of OCs and OC precursors, such as monocytes and macrophages.<sup>8</sup>

Recent studies have highlighted the important roles played by oxidative stress and autophagy in RANKL-induced OC differentiation.<sup>9,10</sup> Several natural compounds, including flavonoids, have been shown to inhibit OC differentiation through their antioxidant activity.<sup>11,12</sup> The regulation of OC formation by the modulation of autophagy has received much attention in recent years. Studies have demonstrated that both chemical and epigenetic regulations can influence OC differentiation.<sup>13,14</sup> Rapamycin, the most common autophagy activator, has been widely used in autophagy research.<sup>15,16</sup> As a highly conserved protein kinase, the mammalian/mechanistic

Received: February 28, 2023

Accepted: May 18, 2023

Published: May 29, 2023



target of rapamycin (mTOR) consists of two structurally and functionally distinct multiprotein complexes named mTORC1 and mTORC2.<sup>17</sup> Of the two, mTORC1 is strongly linked to autophagy and sensitive to rapamycin.<sup>18,19</sup> Inhibition of mTORC1 by rapamycin results in the dephosphorylation of unc-51-like kinase 1 (ULK1) and ULK1-Atg13-FIP200 complex formation, which is essential for autophagosome formation.<sup>17</sup>

However, the role of rapamycin in OC formation and inflammatory musculoskeletal disorders needs to be explored in depth since the results of previous studies have been inconclusive.<sup>20,21</sup> Studies have found that rapamycin attenuates several pathologic changes, with a decrease in levels of oxidative stress.<sup>22,23</sup> To our knowledge, the effect of rapamycin on ROS generation during OC formation has not been reported yet. In addition, during autophagy-regulated processes, it is more reasonable to detect dynamic changes in autophagic flux rather than merely changes in the autophagosome number. However, most of the previous research has focused on the role of rapamycin in the activation of the autophagic pathway, but ignored its effect on autophagy flux during OC differentiation.<sup>16</sup> Hence, we first examined the effect of rapamycin on OC formation *in vitro*, then explored the role of rapamycin in ROS generation and related pathways and its effect on autophagy flux. In addition, a rat model of periodontitis induced by lipopolysaccharide (LPS) was established to explore the effectiveness of rapamycin in treating inflammatory bone loss diseases.

## MATERIALS AND METHODS

**Reagents and Materials.** Dulbecco's modified eagle medium (DMEM), minimum essential medium  $\alpha$  ( $\alpha$ -MEM), and fetal bovine serum (FBS) were purchased from Amizone (USA). 2',7'-Dichlorofluorescein diacetate (DCFH2-DA) kits, monodansylcadaverine (MDC) kits, bicinchoninic acid (BCA) kits, and electron microscope fixatives were purchased from Solarbio (Beijing, China). RANKL, M-CSF, and bovine bone slices were obtained from HUABIO (Hangzhou, China). MitoSOX Red mitochondrial superoxide indicator was obtained from Thermo Fisher Scientific (USA). Antibodies Nrf2, HO-1, GCLC, LC3B, p62, and  $\beta$ -actin were obtained from Proteintech (Wuhan, China). Primers of Cathepsin K (CTSK), tartrate-resistant acid phosphatase 5 (ACP5), nuclear factor of activated T cells 1 (Nfatc1), matrix metalloproteinase-9 (MMP-9), Actb, and the Trizol kit were purchased from Sangon Biotech (Shanghai, China). The goat-anti-rabbit and secondary antibodies were purchased from Bioworld (Nanjing, China). The tartrate-resistant acid phosphatase (TRAP) staining kit was purchased from Sigma (USA). The CCK-8 assay kit was purchased from Biosharp (Guangzhou, China). The Elisa kits for RANKL, OPG (osteoprotegerin), TRACP 5b, TNF- $\alpha$ , IL-1 $\beta$ , and IL-6, as well as the biochemical kits for alkaline phosphatase (ALP), malondialdehyde (MDA), superoxide dismutase (SOD), and nitric oxide (NO), were purchased from Nanjing Jiancheng (Nanjing, China). Rapamycin and bafilomycin A1 were purchased from MedChem Express. *tert*-Butyl hydroperoxide (TBHP) was obtained from Macklin (Shanghai, China). Denosumab was obtained from Selleck (USA). Other reagents were available in our laboratory.

**Cell Culture and Laboratory Animals.** The cell line (RAW264.7) was obtained from Solarbio (Beijing, China) and cultured in DMEM supplemented with 10% FBS at 37 °C

under 5% CO<sub>2</sub> and 95% humidity. We preserved excess cells in our laboratory for future experiments. The primary bone marrow mononuclear cells (BMMs) were obtained after the lysis of red blood cells from the long bones of the C57BL/6 mouse brought from Charles River (Beijing, China) and then cultured in  $\alpha$ -MEM.

Twenty healthy 10 week old male SPF-grade Wistar rats were purchased from Charles River (Beijing, China). The rats were kept at a relative humidity of 50–60% and a temperature of 21–25 °C. The rats in each group had free access to food and drinking water. All animal procedures were carried out in accordance with the guidelines of the Experimental Animal Welfare and Ethics Committee of the Tianjin Institute of Environmental and Operational Medicine.

**In Vitro OC Formation.** RAW264.7 cells were plated into a 24-well plate at a density of  $1 \times 10^4$  cells/well in complete  $\alpha$ -MEM for a day, followed by incubation with RANKL (50 ng/mL) and M-CSF (25 ng/mL). The medium was changed every 2 days in the presence of RANKL (50 ng/mL) and M-CSF (25 ng/mL) to induce the formation of osteoclast-like cells (OCLs).

After being flushed from the mouse bone marrow, all cells were cultured in complete  $\alpha$ -MEM overnight. After red blood cell lysis the next day, the primary BMMs were separated as suspended cells. After cell counting, BMMs were plated into a 24-well plate at a density of  $5 \times 10^4$  cells/well in complete  $\alpha$ -MEM supplemented with M-CSF (40 ng/mL) for a day, followed by the addition of RANKL (50 ng/mL) on the second day. The solution was changed after 2 days in the presence of RANKL (50 ng/mL) and M-CSF (25 ng/mL). For rapamycin treatment, cells were incubated in the presence of different concentrations (50/100/200 nM) of rapamycin for 5 consecutive days since studies used 100 nM rapamycin in RAW 264.7 cells for induction of autophagy.<sup>24,25</sup> For TBHP treatment, the cells were treated with distinct concentrations (20/50/100  $\mu$ M) of TBHP, after 2 days of induction with RANKL for 4 h. For bafilomycin A1 treatment, the cells were incubated with 20 nM bafilomycin A1 for 4 h before sample collection. We collected cell samples for further experiments after 5 days of induction with RANKL.

**Cell Viability Assay.** The cytotoxicity of rapamycin was detected by the CCK-8 assay during OC differentiation or normal culture. After 5 days of culture, the medium was changed, and 10  $\mu$ L of CCK-8 buffer was added, followed by incubation in darkness at 37 °C for 1 h. The absorbance was measured at 450 nm by a microplate reader (Molecular Devices, USA).

**TRAP Staining.** Briefly, after 5 days of OCL and OC induction, the cells were fixed in 4% paraformaldehyde for 3 min. TRAP staining was performed for OC detection according to the manufacturer's protocol. At least six random images were captured for each well using a fluorescence microscope (Leica, Germany). Lastly, TRAP-positive cells (purple) with no fewer than five nuclei were counted as OCLs or OCs.

**Determination of the Level of Oxidative Stress by the MitoSOX Assay and the H2DCFH-DA Assay.** Mitochondrial superoxide ion production was assayed using a MitoSOX Red mitochondrial superoxide indicator. Intracellular ROS was detected by the fluorescent probe 2',7'-dichlorofluorescein diacetate (H2DCF-DA). Both assays were carried out according to the manufacturer's protocol.

Table 1. Primer Sequences for Real-Time PCR

gene	forward primer, 5' to 3'	reverse primer, 5' to 3'
CTSK	GAAGAAGACTCACCAGAAGCAG	TCCAGGTTATGGGCAGAGATT
ACPS	CACTCCCACCCTGAGATTTGT	CATCGTCTGCACGGTTCTG
Nfatc1	GACCCGGAGTTCCGACTTCG	TGACACTAGGGGACACATAAAGT
MMP-9	CTGGACAGCCAGACACTAAAG	CTCGCGCAAGTCTTCAGAG
Actb	GGCTGTATTCCCCTCCATCG	CCAGTTGGTAAACATGCCATGT

**Monodansylcadaverine Stain.** Autophagic staining was measured using a cell monodansylcadaverine (MDC) assay kit (Solarbio, Beijing, China) according to the manufacturer's protocol.

**Western Blot Analysis.** Briefly, treated OCs were lysed in RIPA buffer supplemented with phenylmethylsulfonyl fluoride and phosphatase inhibitors. Whole cell lysates were separated using 4–12% or 15% SDS-PAGE and transferred onto polyvinylidene difluoride membranes (Bio-Rad system). The membranes were blocked with 5% non-fat milk in Tris buffered saline with Tween 20 (20 mM Tris–HCl, 500 mM NaCl, and 0.1% Tween 20) at room temperature for 2 h. They were subsequently incubated with targeted primary antibodies overnight and, subsequently, with the corresponding secondary antibodies. Finally, the chemiluminescence signals were captured with an Amersham Imager 680 (USA).

**Quantitative PCR.** Total RNA was extracted from BMMs and RAW 264.7 cells after OC formation using a Trizol kit, following a standard protocol. cDNA was obtained through reverse transcription from an aliquot of 500 ng of RNA, by TaKaRa PrimeScript Reverse Transcriptase (TaKaRa Bio Inc., Shiga, Japan). Quantitative PCR was performed using the SYBR green mixture (Takara) to detect the expression of genes. The  $2^{-\Delta\Delta CT}$  method was used to analyze results in which data were normalized using the relative expression of ACTB as a control. The primer sequences are shown in Table 1.

**Bone Resorption Measurement.** BMMs were seeded on the bovine bone slice and induced with the RANKL and MCSF mentioned above for 7 days. Then, the slice will be fixed and detected by scanning electron microscopy (HITACHI, Japan).

**Rat LPS-Induced Periodontitis Model.** After adjustable feeding for 3 days, a total of twenty 10 week old healthy Wistar male rats were randomly allocated into four groups ( $n = 5$ ) to establish the LPS-induced periodontitis rat model.<sup>26</sup> control (treated with phosphate buffered saline), model group (treated with 1 mg/mL of LPS), low-dose rapamycin (treated with 1 mg/mL of LPS and 42 ppm of rapamycin), and high-dose rapamycin (treated with 1 mg/mL of LPS and 160 ppm of rapamycin). The choice of low-dose rapamycin referred to a published periodontitis animal study,<sup>27</sup> and the choice of high-dose rapamycin was consistent with an in vitro study (160 ppm rapamycin  $\approx$  200 nM rapamycin).

Each rat was anesthetized by intraperitoneal injection of 2% pentobarbital (40 mg/kg), followed by an injection of LPS (containing 0/42/160 ppm of rapamycin) dissolved in normal saline into the vestibular, lingual gingiva of the maxillary first molar, and the gingiva between the first and second molars (20  $\mu$ L solution for each injection site) on both sides in all groups except the control group (which was injected with the same amount of normal saline). LPS was injected every other day for 4 weeks during the entire course of the experiment.

**Therapeutic Efficacy In Vivo.** High-resolution micro-computed tomography ( $\mu$ CT) (PerkinElmer, USA) (90 Kv, 180 mA, equidistant resolution 20  $\mu$ m, exposure time 4.5 min) was used to examine the fixed alveolar bone. Briefly, after fixing, the alveolar bones were decalcified and embedded in paraffin. Thereafter, we performed TRAP and hematoxylin–eosin (HE) for morphometric observation. The serum was collected for ELISA and the biochemical assay. The levels of RANKL, OPG, TRACP5b, TNF- $\alpha$ , IL-1 $\beta$ , and IL-6 in the serum were determined by the ELISA assay. Biochemical kits were used to test the enzyme activities of ALP, MDA, SOD, and NO. A multifunctional microplate reader (Molecular Devices, USA) was used to measure the serum indicators. All procedures were performed in accordance with the manufacturer's instructions.

**Statistics.** The data were expressed as the means  $\pm$  standard deviation. Independent sample t-tests were used for the comparison of two groups. For multiple comparisons, a one-way analysis of variance (ANOVA) was performed. Values of  $p < 0.05$  were considered statistically significant. Data analyzes were performed using GraphPad Prism 8.4.0.

## RESULTS

**Rapamycin Inhibited RAW 264.7 Cells and BMMs OC Differentiation in a Concentration-Dependent Manner In Vitro.** The viability of RAW 264.7 cells did not change significantly under rapamycin treatment, regardless of differentiation or not, sd measured by a CCK-8 assay (Figure 1A). The number and size of TRAP-positive OCs were significantly decreased after treatment with rapamycin in a dose-dependent manner (Figure 1B–D). In addition, an increase in the rapamycin concentration in BMMs led to the downregulation of the mRNA levels of mature OC function-related markers, such as ACP5, CTSK, Nfatc1, and MMP-9 (Figure 1E). In addition, rapamycin exhibits inhibitory effects similar to those of denosumab (Figure 1B–E). These results demonstrated that rapamycin could significantly inhibit OC formation with little or no evident cytotoxicity.

**Rapamycin Suppressed the Level of Oxidative Stress by Upregulating the Nrf2/GCLC Signaling Pathway in a Dose-Dependent Manner during Osteoclastogenesis.** Rapamycin significantly inhibited the level of oxidative stress (Figure 2A–D), in a dose-dependent manner. Rapamycin did not affect the fluorescence intensity of MDC staining, which was positively associated with the number of autolysosomes (Figure 2E,F). A Western blot was performed to explore the mechanism of ROS suppression and the influence of rapamycin on autophagy. Previous studies have demonstrated the downregulation of Nrf2, a key transcription factor regulating the antioxidant response, during RANKL-induced osteoclastogenesis. In the present study, the level of Nrf2 was rescued by rapamycin in a dose-dependent manner during OC formation (Figure 2G,H). Furthermore, the classical downstream signaling molecules of Nrf2 were obviously changed by



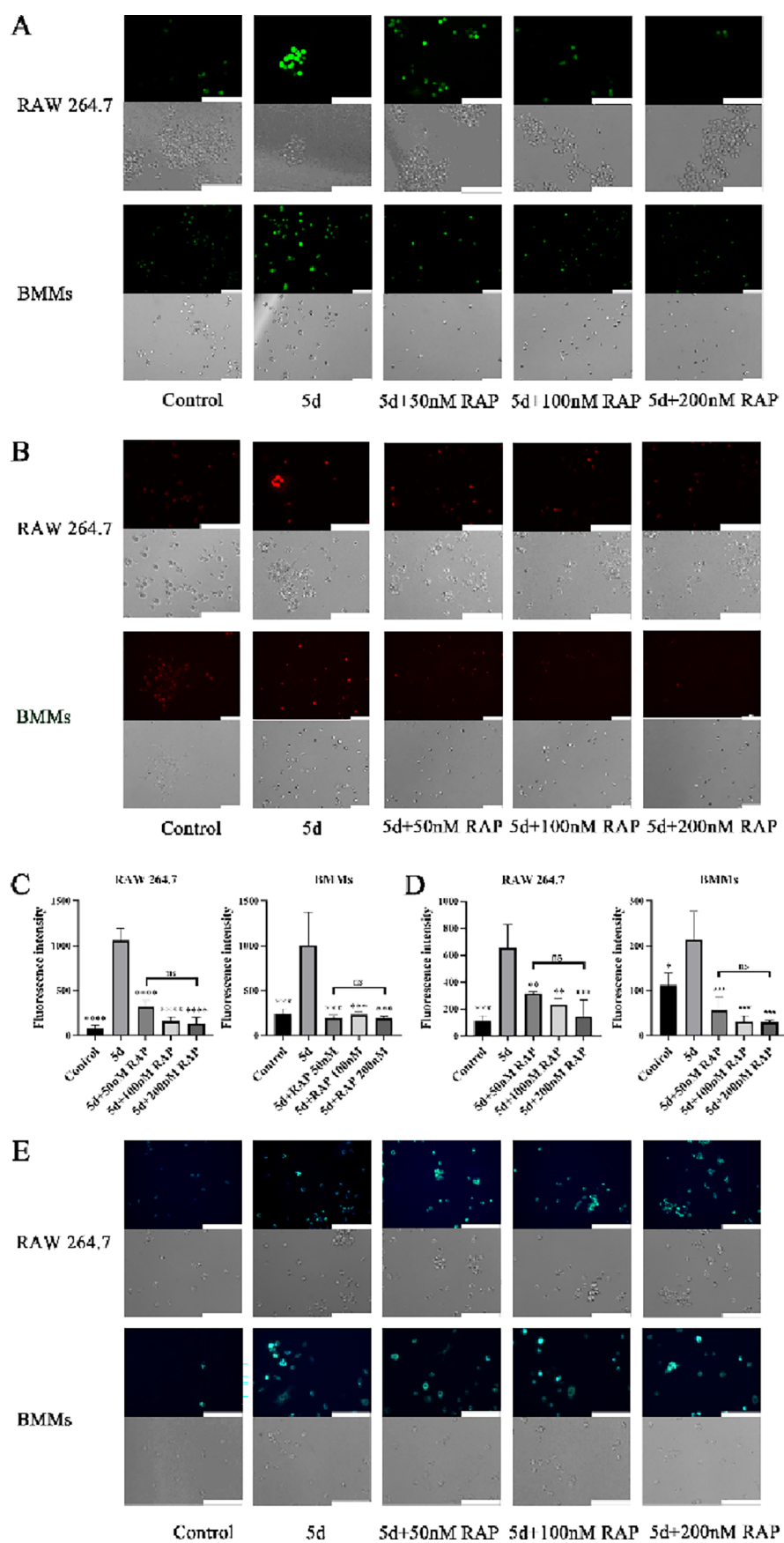
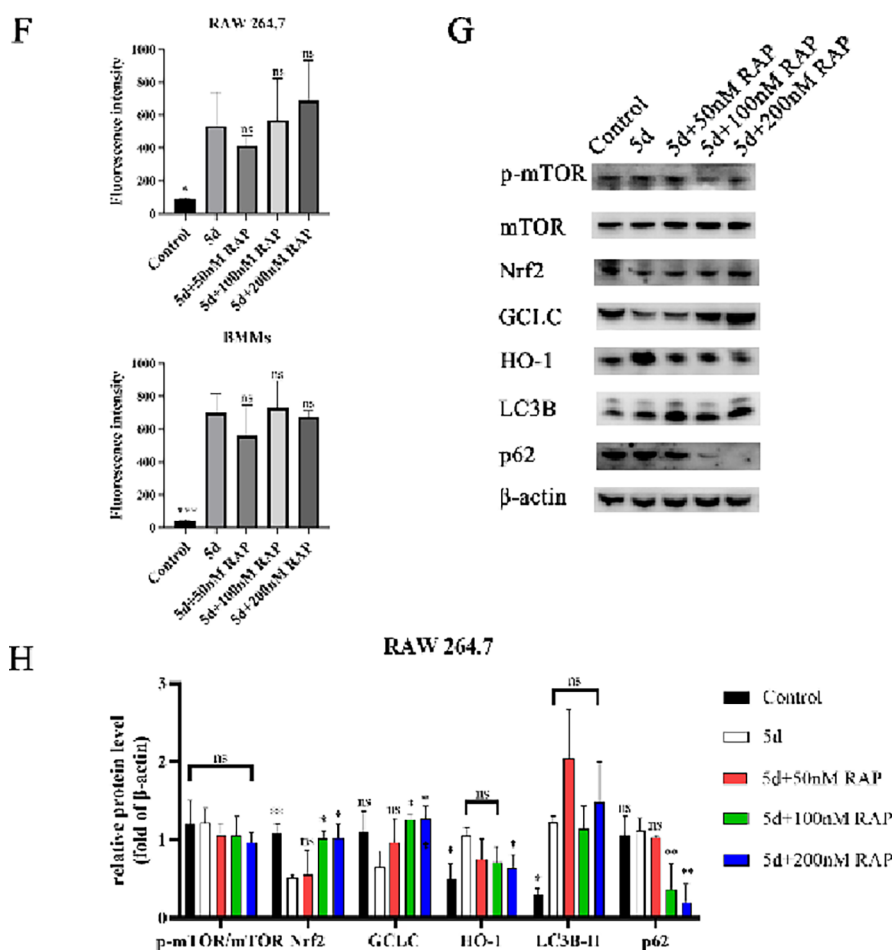


Figure 2. continued



**Figure 2.** Rapamycin significantly suppressed the level of oxidative stress during OC formation and upregulated the Nrf2/GCLC signaling pathway in RAW 264.7 cells in a dose-dependent manner. (A) ROS levels in RAW 264.7 cells and BMMs using DCFH2-DA. Scale bar: 100  $\mu$ m. (B) Mitochondrial superoxide levels in RAW 264.7 cells and BMMs using MitoSOX. Scale bar: 100  $\mu$ m. (C) Quantitative analysis of DCFH2-DA fluorescence intensity. (D) Quantitative analysis of MitoSOX fluorescence intensity. (E) Autophagy level in RAW 264.7 cells and BMMs using MDC. Scale bar: 100  $\mu$ m. (F) Quantitative analysis of MDC fluorescence intensity. (G) Expression levels of p-mTOR, mTOR, Nrf2, GCLC, HO-1, LC3B, and p62, relative to  $\beta$ -actin, in RAW 264.7 cells in the presence of 0/50/100/200 nM rapamycin, after 5 days of OC differentiation. (H) Protein intensity was analyzed by Image J software. (C, D, F, H)  $n = 3$ ; versus the 5 day RANKL-induced group; ns, no significance, \* $P < 0.05$ , \*\* $P < 0.01$ , \*\*\* $P < 0.001$ , and \*\*\*\* $P < 0.0001$ .

lated under rapamycin treatment, while rapamycin caused a marked increase in the degradation of autophagy substrate p62 in a concentration-dependent manner. The ratio of p-mTOR/mTOR only slightly decreased in the presence of rapamycin (with no statistical difference). These results indicate that rapamycin might not only increase autophagosome formation but also increase autophagy flux during osteoclastogenesis. In addition, since intracellular ROS is an essential trigger of autophagy and is involved in the activation of the AMPK pathway, we found that the ratio of p-AMPK/AMPK decreased in the presence of rapamycin (Supporting Information Figure 1).

**Rapamycin Inhibited OC Formation and Function by Oxidative Suppression.** TBHP was applied to reverse the oxidative suppression of OCs during rapamycin treatment to explore the role of oxidative suppression by rapamycin. The CCK-8 assay was performed to determine the optimal dose of TBHP. The CCK-8 assay was performed to determine the optimal dose of TBHP. No significant damage effects were observed after 4 h of treatment with 20 or 50  $\mu$ M TBHP, respectively (Figure 3A,B). Thereafter, pre-treatment with 20 and 50  $\mu$ M TBHP was performed for 4 h to reduce the

oxidative stress level suppressed by rapamycin, which was measured by the MitoSOX assay and DCFH2-DA. The pre-treatment reduced the oxidative stress level in the 200 nM rapamycin group (Figure 3C–E). Four hours of pre-treatment with 20 and 50  $\mu$ M TBHP reversed the suppression effect of rapamycin in OC differentiation, as shown by the increase in the number of TRAP-positive cells detected by TRAP stain (Figure 3F,G). Pre-treatment with TBHP also reversed the decrease in the mRNA expression levels of mature OC functional markers by rapamycin, such as CTSK and ACP5 (Figure 3H). The effect of rapamycin on bone resorption was determined by bone resorption measurements. Scanning electron microscopy showed that 200 nM rapamycin impaired bone resorptive function, while 20  $\mu$ M TBHP could restore the resorption ability to a certain extent (Figure 3I,J). All these results indicated that rapamycin could suppress OC formation via downregulation of the oxidative stress level.

**Rapamycin Increased Autophagy Flux during OC Formation and Suppressed the Level of Oxidative Stress via the Autophagy-Mediated Pathway during OC Formation.** To further elucidate the precise effect of rapamycin-enhanced autophagic activity and to comprehen-

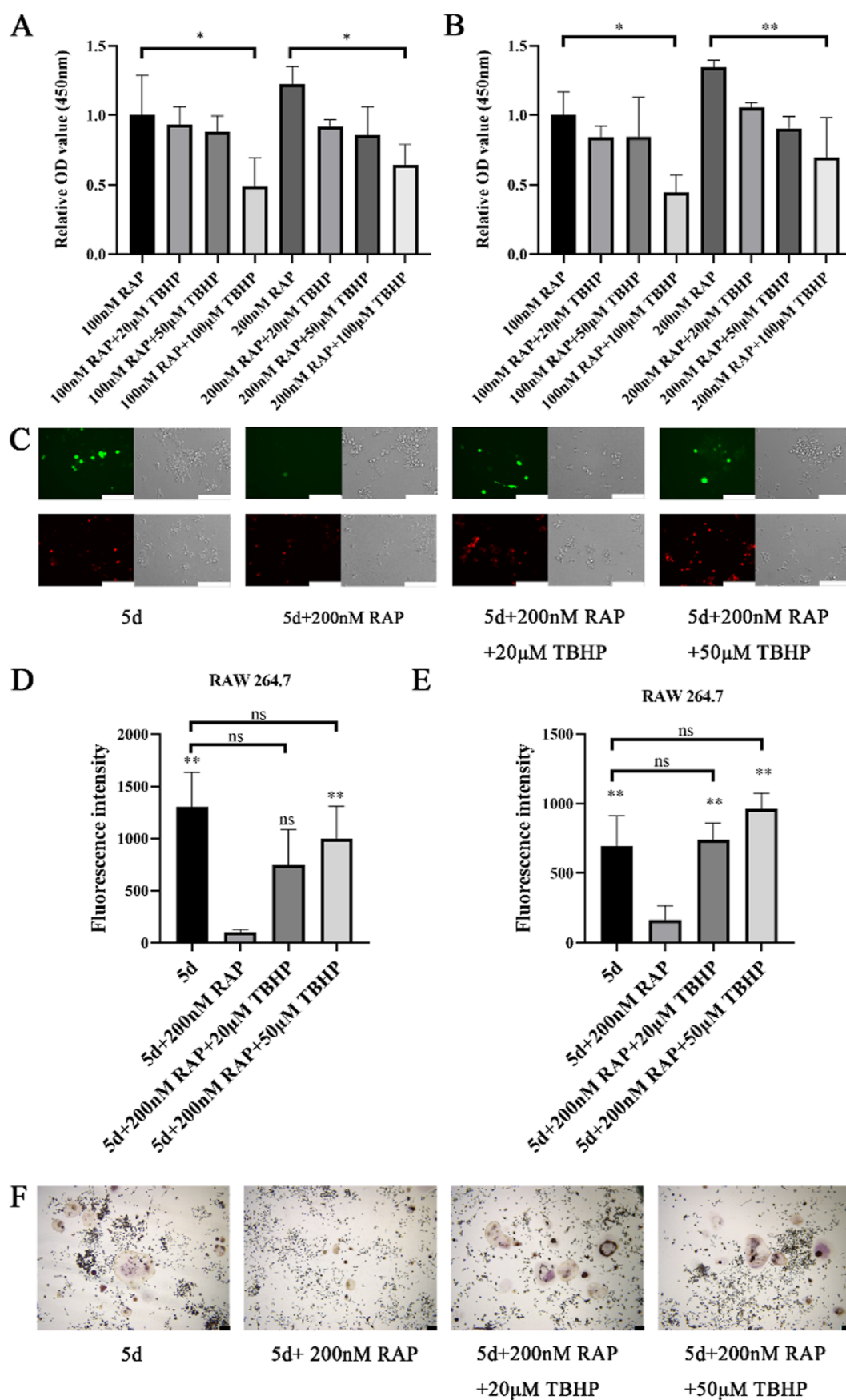
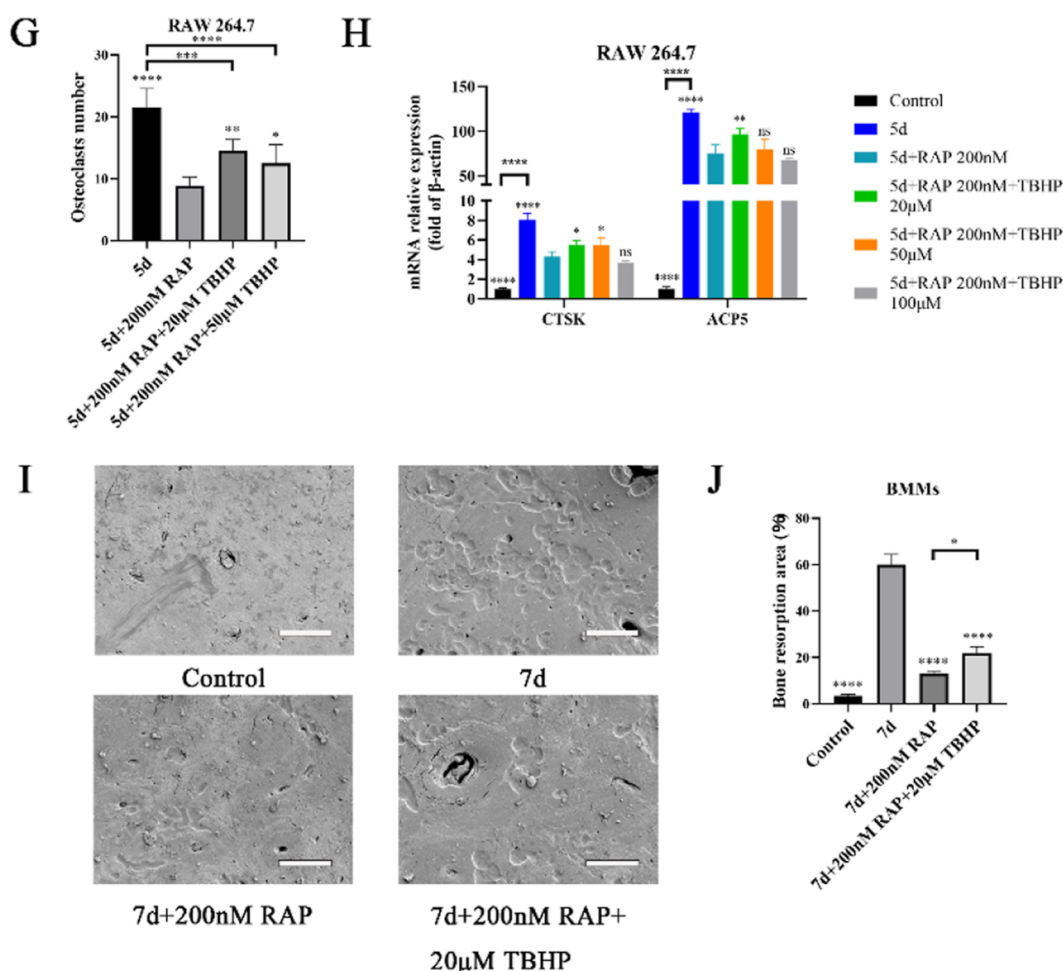


Figure 3. continued



**Figure 3.** Rapamycin inhibits OC formation and function by oxidative suppression. (A,B) The cytotoxicity of TBHP in the presence of rapamycin with/without RANKL stimulation.  $n = 3$ ; versus 100/200 nM rapamycin; ns, no significance,  $*P < 0.05$ ,  $**P < 0.01$ . (C) ROS levels and superoxide levels in RAW 264.7 cells in the presence of TBHP and rapamycin during RANKL stimulation. Scale bar: 100  $\mu\text{m}$ . (D,E) Quantitative analysis of DCFH2-DA and MitoSOX fluorescence intensity.  $n = 3$ ; versus 5 days of induction with 200 nM rapamycin; ns, no significance,  $**P < 0.01$ . Scale bar: 100  $\mu\text{m}$ . (F) TRAP staining of the RAW 264.7 cells. Scale bar: 100  $\mu\text{m}$ . (G) Quantitative analysis of the number of multinuclear cells of mature OC from RAW 264.7 cells.  $n = 6$ ; versus 5 days of induction with 200 nM rapamycin;  $*P < 0.05$ ,  $**P < 0.01$ ,  $****P < 0.0001$ . (H) OC mature and functional genes of RAW 264.7 cells treated with or without 20/50  $\mu\text{M}$  TBHP in the presence or absence of 200 nM rapamycin for 5 days.  $n = 3$ ; versus 5 days of induction with 200 nM rapamycin;  $*P < 0.05$ ,  $**P < 0.01$ ,  $****P < 0.0001$ . (I) Representative images of bone resorption measurement. Scale bar: 100  $\mu\text{m}$ . (J) Quantitative analysis of bone resorption area.  $n = 3$ ; versus 7 days induction group;  $*P < 0.05$ ,  $****P < 0.0001$ .

sively evaluate changes in autophagy flux, the LC3 protein flip test and expression of soluble/insoluble p62 were performed together.<sup>28</sup> Typically, when bafilomycin A1 is applied to determine the effect of drugs on autophagic flux, four groups are routinely established: a 5 days differentiation group (5d), a 5 day differentiation combined bafilomycin A1 treatment group (5d + BAF), a 5 day differentiation group combined rapamycin treatment group (5d + RAP), and a 5 days differentiation group combined rapamycin and bafilomycin A1 treatment group (5d + RAP + BAF). As depicted in Figure 4A,B, western blot showed that both rapamycin and rapamycin plus bafilomycin A1 groups significantly increased the transformation of LC3I to LC3II. Analysis of the levels of soluble and insoluble p62 showed that the degradation rate of soluble p62 was much higher in the rapamycin group than in the normal differentiation group (Figure 4A–D), while the levels of insoluble p62 were similar in both groups. Hence, rapamycin increased the amount of autophagosome formation and autophagic flux. To clarify the relationship between the

antioxidant effect and autophagy flux increased by rapamycin, DCFH2-DA and MitoSOX assays were performed to investigate whether the blocking of autophagy flux would increase ROS levels. Both assays showed that the inhibition of autophagy flux by bafilomycin A1 did not lead to an increase in ROS levels during RANKL-induced OC formation. However, when the autophagy flux was blocked by bafilomycin A1 in the rapamycin treatment group, which had been increased by rapamycin, the level of oxidative stress was significantly increased (Figure 4E–H). These results indicated that the antioxidant effect of rapamycin during OC formation was mediated by increased autophagy flux.

**Rapamycin-Attenuated LPS-Induced Rat Periodontitis and Alveolar Bone Erosion.** A LPS-induced rat periodontitis model was established to investigate the potential of rapamycin in the treatment of inflammatory bone-related diseases. The brief experimental design and procedure for periodontitis establishment and rapamycin intervention are depicted in Figure 5A. Micro-CT results revealed that the

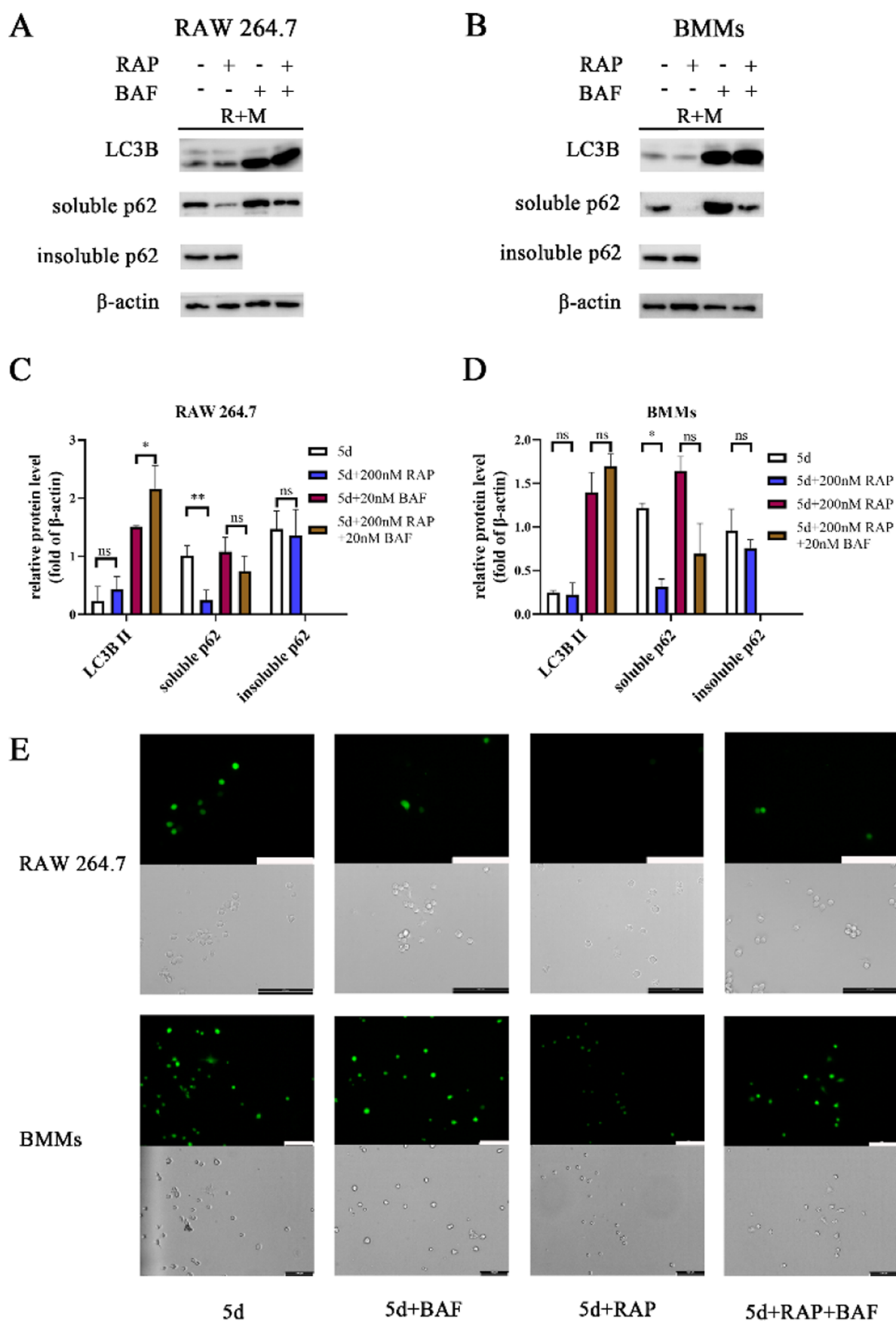
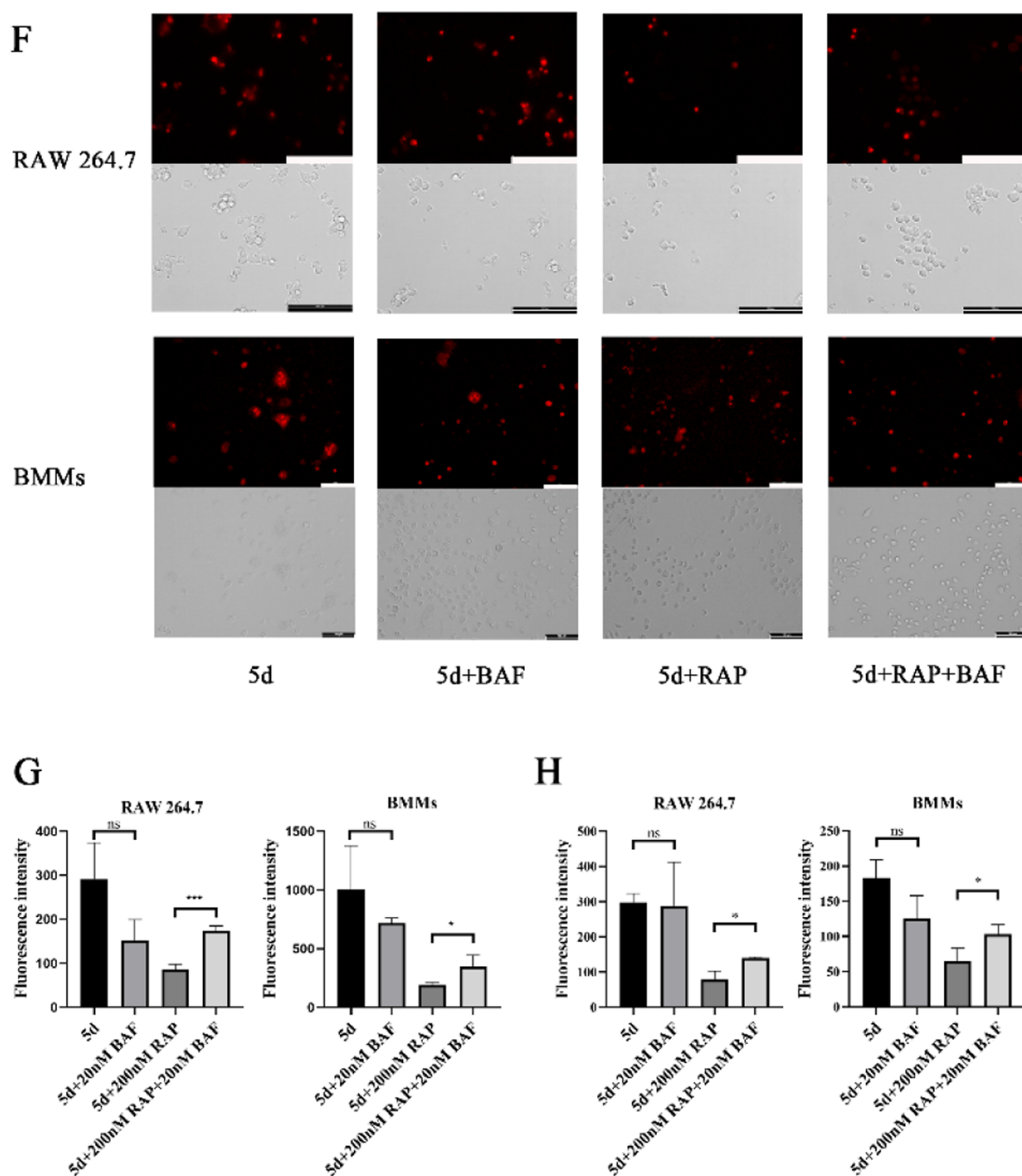


Figure 4. continued



**Figure 4.** Rapamycin increased autophagy flux and suppressed the level of oxidative stress via the autophagy-mediated pathway during OC formation. (A,B) Representative images of protein expression of LC3B, soluble p62, and insoluble p62 in BMMs by the LC3 protein flip test. (C,D) Quantitative analysis of protein intensity of LC3B, soluble p62, and insoluble p62 relative to  $\beta$ -actin in RAW 264.7 cells and BMMs.  $n = 3$ ; ns, no significance,  $*P < 0.05$  and  $**P < 0.01$ . (E,F) ROS and mitochondrial superoxide levels in RAW 264.7 cells and BMMs using DCFH2-DA and MitoSOX. Scale bar: 100  $\mu\text{m}$ . (G, H) Quantitative analysis of DCFH2-DA and MitoSOX fluorescence intensity.  $n = 3$ ;  $*P < 0.05$ ,  $***P < 0.001$ .

alveolar bone around the maxillary molars was significantly reduced after LPS injection. The distance from the cemento-enamel junction (CEJ) to the alveolar bone crest (ABC) of the maxillary first molar increased significantly as compared to the control group, which confirms the establishment of experimental periodontitis in our laboratory model (Figure 5B). CT analysis showed a marked bone loss in the model group, with a decrease in the trabecular number (Tb. N) and thickness (Tb. Th), accompanied by an increase in trabecular separation (Tb. Sp) when compared to the control

group (Figure 5B,C). Rapamycin treatment rescued bone loss and decreased the distance of CEJ to ABC (Figure 5B,C), thus decreasing alveolar erosion and reversing the trabecular parameters when compared to the model group. The high-dose rapamycin group showed a better therapeutic effect as compared to the low-dose group (Figure 5B,C). HE staining showed typical pathologic changes in the model group, such as inflammatory cell infiltration, hyperplasia, and erosion of the surface of the crest, while rapamycin treatment diminished these pathologic changes. Again, the high-dose group showed a

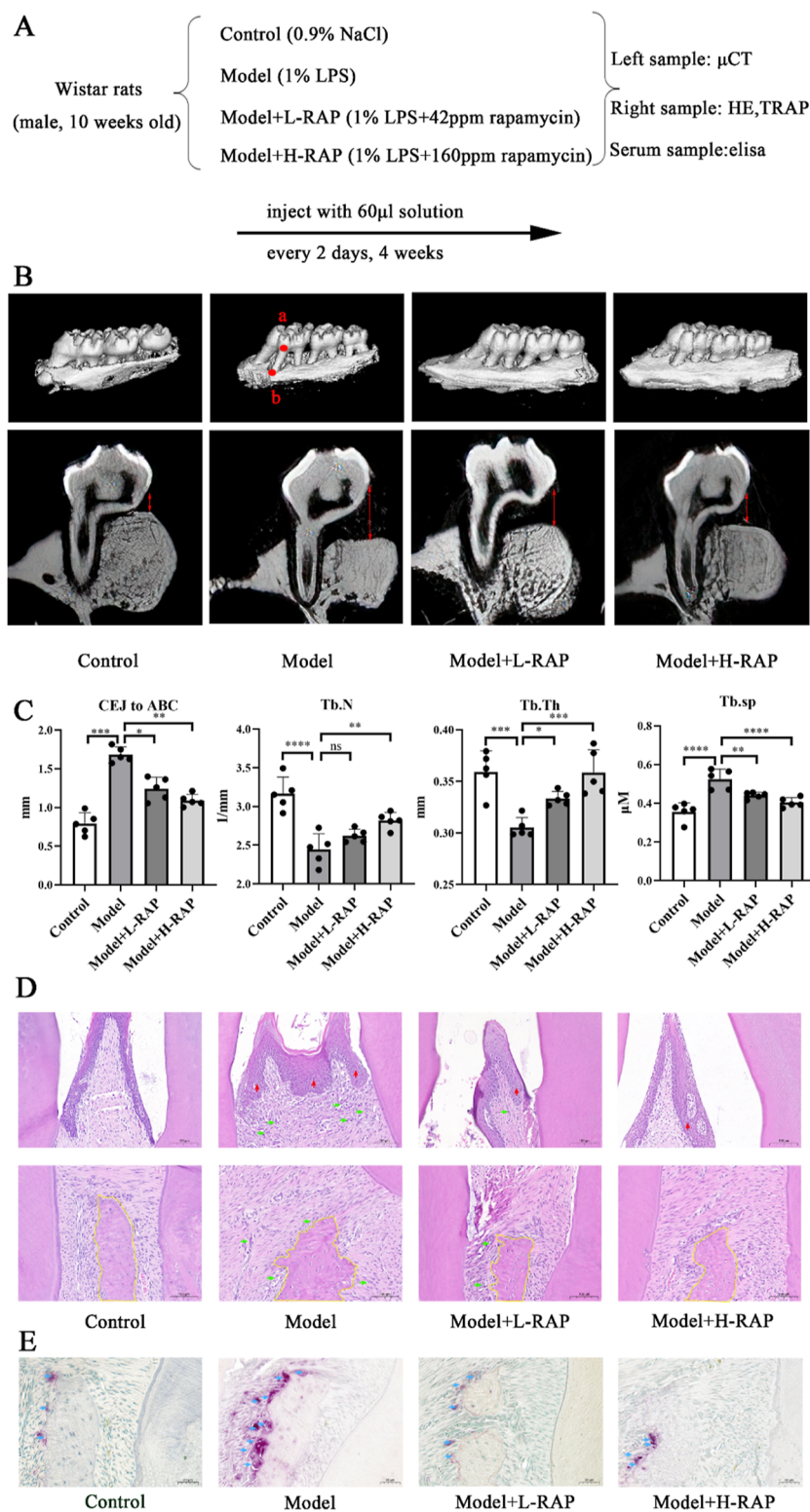


**Figure 5.** Rapamycin attenuated LPS-induced rat periodontitis and alveolar bone erosion. (A) Experimental design. (B) Reconstruction of alveolar bone using  $\mu$ CT and representative slices from the first molar in the coronal plane of control rats with periodontitis with saline (model), periodontitis with 42 ppm rapamycin (low-dose) and with 160 ppm rapamycin (high-dose). (a) CEJ; (b) ABC. The red arrow represents the distance from CEJ to ABC. (C) Quantitative analysis of the CEJ to ABC and bone trabecula bone parameters, such as Tb. N, Tb. Th and (Tb. Sp).  $n = 5$ ; versus The model group; \* $P < 0.05$ , \*\* $P < 0.01$ , \*\*\* $P < 0.001$ , and \*\*\*\* $P < 0.0001$ . (D) Histopathologic findings in periodontitis lesions (red arrows, hyperplasia of the gingival epithelium with the formation of rete pegs; green arrows, moderate mononuclear inflammatory cell infiltration; yellow lines, alveolar bone surfaces of the ABC. scale bar: 100 $\mu$ m). (E) TRAP staining results (the blue arrows represent OCs); scale bar: 50  $\mu$ m.

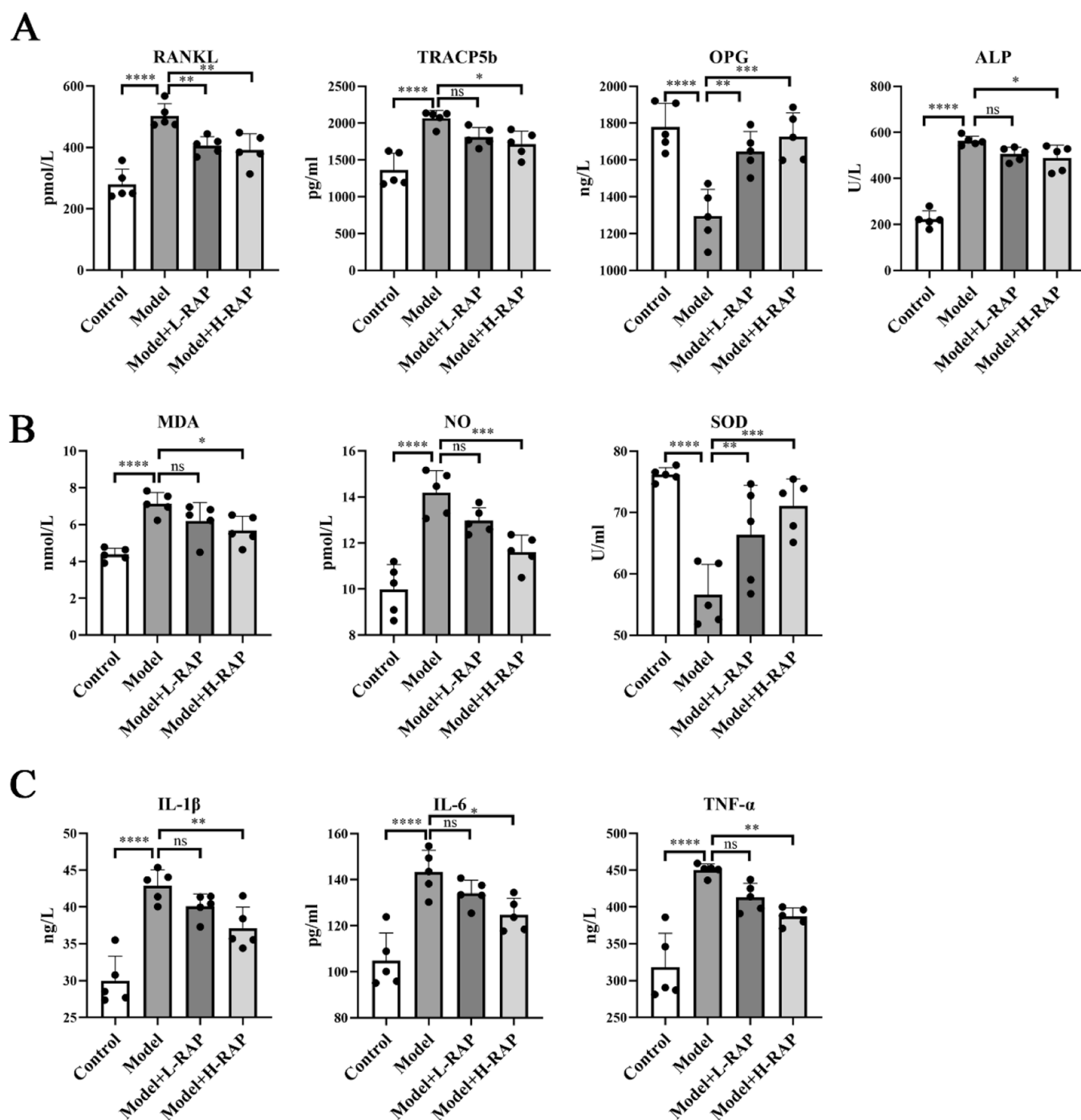


**Figure 6.** Rapamycin alleviates the bone resorption serum indicator associated with periodontitis in vivo and decreases the level of oxidative stress and inflammatory factor secretion. (A) Serum levels of RANKL, OPG, TRACP5b, and ALP. (B) Total MDA, SOD, and NO of rat serum. (C) Serum levels of IL-1 $\beta$ , IL-6, and TNF- $\alpha$ . (A, B, C)  $n = 5$ , versus model group; \* $P < 0.05$ ; \*\* $P < 0.01$ ; \*\*\* $P < 0.001$ ; and \*\*\*\* $P < 0.0001$ .

better protection effect than the low-dose group (Figure 5D). TRAP staining showed that the model group had more OCs with larger cell morphology, and the rapamycin group reduced OC formation (Figure 5E). These data demonstrated that the high-dose rapamycin group was more efficient than the low-dose group, with fewer OC formation and less bone erosion measured, and fewer pathological changes (hyperplasia and inflammatory cell infiltration).

**Rapamycin Alleviated the Bone Resorption Serum Indicator Associated with Periodontitis in Vivo and Decreased the Level of Oxidative Stress and Inflammation**

**Factor Secretion.** As explicitly shown in Figure 6A, the serum levels of bone resorption biomarkers, such as TRACP5b, RANKL, and ALP, were significantly increased in the model group, which is indicative of osteoclastogenesis enhancement and osteogenesis repair, while a decrease was observed in OPG, which is an OCs' suppression cytokine. Rapamycin treatment could effectively reverse the levels of these biomarkers in both high- and low-dose groups compared to the model group (Figure 6A). While the high-dose rapamycin group was also found to suppress the serum levels of pro-inflammatory cytokines, such as IL-6, IL-1 $\beta$ , and TNF-

$\alpha$ , as well as the oxidative stress level measured by MDA and NO, the level of the anti-oxidative stress indicator SOD increased. However, no significant difference was found in the low-dose group compared to the model group (Figure 6B,C) regarding pro-inflammatory and the oxidative stress serum detection index.

## DISCUSSION

Elevated level of local oxidative stress leads to the excessive activation of OC differentiation, which is the major cause of many bone loss diseases. To the best of our knowledge, this study is the first to demonstrate that rapamycin, the most common autophagy activator, has therapeutic potential in bone loss diseases and inhibits osteoclastogenesis in both RAW 264.7 cells and BMMs in vitro through the antioxidative effect.

Mitochondria are the most important ROS source in the OC differentiation process. Intracellular ROS have been regarded as essential molecules for osteoclastogenesis, which is usually detected by DCFH2-DA.<sup>29</sup> In the current study, we also found an increase in the mitochondrial anionic superoxide level during OC differentiation, as detected by MitoSOX, which has seldom been reported in OC-related studies. Previous studies demonstrated that the suppression of oxidative stress during OC formation would inhibit OC-specific transcription factors, such as Nfatc1 and C-FOS, thus impairing OC differentiation and function.<sup>30,31</sup> We observed that rapamycin impaired OC differentiation and function by suppressing both intracellular ROS and mitochondrial superoxide levels. In addition, we demonstrated that the antioxidant pathway, such as Nrf2/GCLC, was upregulated by rapamycin in an obvious concentration-dependent manner.<sup>32</sup> We further showed that exogenously generated intracellular H<sub>2</sub>O<sub>2</sub> (TBHP) rescued OC differentiation and function in the presence of rapamycin. Collectively, the data demonstrated that rapamycin has a nonnegligible anti-oxidative effect rather than simple mTOR pathway inhibition or autophagy activation. Application of rapamycin should be cautious, especially in both oxidative stress and autophagy-related cellular processes such as OC differentiation.

As a vital eukaryotic signaling network coordinator, mTOR protein kinases regulate cell growth in response to environmental factors. Previous studies have demonstrated that both epigenetic and chemical regulation of mTORC1 influenced the formation of OCs in vitro and the progression of the hard tissue disease, although several questions remain. For example, Zhang et al.<sup>20</sup> found that targeted knock-out of Raptor (a key component of mTORC1) resulted in mice with osteopenia and enhanced osteoclastogenesis, while targeting deletion of Tsc1 (a negative regulator of mTORC1) showed the opposite effect. However, Dai et al.<sup>21</sup> revealed that mTORC1 prevented the differentiation of OC precursors in vitro and in mice by the inhibition of NF- $\kappa$ B/Nfatc1 signaling. Further studies have demonstrated the dual roles of mTORC1 in osteoclastogenesis and the dose-dependent effects of rapamycin on bone homeostasis.<sup>33</sup> It should be noted that while these studies have shed light on the mechanisms related to the mTOR signaling pathway, they have not taken into account the antioxidative stress impact of rapamycin. Our study demonstrated that rapamycin could inhibit osteoclastogenesis by significantly suppressing the level of oxidative stress.

In recent years, autophagy has been found to participate in several bone-related diseases and osteogenesis/osteoclastogenesis. As the most common autophagy activator, rapamycin

has been widely used in OC and autophagy-related studies.<sup>14,34</sup> However, to the best of our knowledge, those studies have used rapamycin as a simple autophagy activator but neglected its effect on autophagy flux and oxidative stress. For the first time, our research has shown that the common autophagy activation dose of rapamycin (200 nM or so) not only increased the number of autophagosomes but also increased the autophagy flux during OC differentiation in vitro, which may involve lysosome changes. The autophagic process could relieve oxidative stress, which was proved by numerous studies.<sup>35,36</sup> Due to the complex crosstalk between ROS and autophagy,<sup>35–37</sup> we designed several experiments to further explore their interactions. Bafilomycin A1 was applied to block the autophagy flux. The results showed that blocking autophagy for 4 h by bafilomycin A1 could not induce an increase in the level of oxidative stress during OC formation (without rapamycin). But the same application induced oxidative stress increase in the presence of rapamycin. These results indicated that the antioxidative effect of rapamycin was related to the increase in autophagy flux. Second, the ROS level is an important trigger of autophagy, especially when it involves the activation of the AMPK signaling pathway.<sup>38,39</sup> Previous autophagy-related studies have only used rapamycin as an autophagy activator but ignored its antioxidative stress effect and its influence on the AMPK signaling pathway during osteoclastogenesis.<sup>14</sup> Our study demonstrated that rapamycin could downregulate the expression of *p*-AMPK, which could explain the absence of a significant reduction in the ratio of *p*-mTOR/mTOR under rapamycin treatment during osteoclastogenesis.

Also, as the famous anti-aging drug, rapamycin only caused reversible adverse effects after ending treatment, and it has been tested in many organs, which indirectly proved its safety.<sup>40</sup> A previous study reported the use of rapamycin as an anti-aging drug to treat elderly mice periodontitis.<sup>27</sup> Tissue regeneration with rapamycin was performed several months after periodontitis was established, emphasizing the role of rapamycin in osteogenesis. It demonstrated that rapamycin could regenerate the periodontal bone and attenuate gingiva and periodontal bone destruction in long-term chronic bone disease.<sup>27</sup> In this study, a short-term LPS-induced periodontitis model was established, and rapamycin was applied from the beginning to focus on the effect of rapamycin on osteoclastogenesis. The results of  $\mu$ -CT, HE staining, and TRAP staining showed that low- and high-dose rapamycin could protect alveolar bone from erosion, reduce the distance between the CEJ and the ABC, and diminish the pathologic changes around periodontal tissue. The high-dose group had a better protective effect as compared to the low-dose group. Serum assays showed a decrease in bone resorption indicators, such as RANKL and TRACP5b, in the rapamycin treatment group.

To further explore the mechanism of rapamycin in treating periodontitis, oxidative stress and inflammatory markers were examined. As proinflammatory cytokines, IL-6 and TNF- $\alpha$  enhance osteoclastogenesis and directly and indirectly induce excessive OC formation by aggravating local tissue oxidative stress.<sup>38,39</sup> Therefore, therapeutic drugs either block the OC directly or do so indirectly via cytokine arrest.<sup>41,42</sup> However, compared to the model group, only the high-dose rapamycin treatment group showed greater suppression of the common inflammatory and proinflammatory factors,<sup>43,44</sup> such as IL-1 $\beta$ , TNF- $\alpha$ , and IL-6. Similarly, biochemical results indicated that only high-dose rapamycin could significantly inhibit oxidative

stress injuries, such as MDA and NO reduction and SOD enhancement, when compared to the model group. Based on these data, we speculated that the high dose of rapamycin could directly inhibit OC formation as well as indirectly inhibit OC via suppression of the level of inflammatory cytokines and oxidative stress in the local tissue.<sup>45</sup>

Many studies have found that some natural extracts could also inhibit LPS-induced bone loss by ROS suppression, such as Alpinetin, Oroxylin A, Diosmetin, etc.<sup>46–48</sup> It is valuable to compare the efficacy, safety, and mechanism of action of rapamycin with those of these compounds. The exact mechanism by which rapamycin regulates immune response and alleviates oxidative stress in vivo is still unclear, whether via immunosuppression<sup>49</sup> or the autophagy pathway,<sup>50</sup> since rapamycin is regarded as both an autophagy activator and an immunosuppressor. The complex interactions between immune response, autophagy, and oxidative stress need to be further elucidated, especially in these inflammatory bone diseases.

In summary, we revealed, for the first time, that rapamycin inhibited OC differentiation by the suppression of oxidative stress and explored the interactions between ROS and autophagy flux when rapamycin was applied during OC formation. An animal model of periodontitis induced by LPS demonstrated the therapeutic potential of rapamycin for inflammatory bone-loss diseases. Future studies should focus on exploring the complex interactions between autophagy and oxidative stress in inflammatory bone disease.

## ■ ASSOCIATED CONTENT

### SI Supporting Information

The Supporting Information is available free of charge at <https://pubs.acs.org/doi/10.1021/acsomega.3c01289>.

Expression of *p*-AMPK and AMPK after 5 days' OC formation in the presence of 0/100/200 nM rapamycin in BMMs (PDF)

## ■ AUTHOR INFORMATION

### Corresponding Authors

**Xin-Xing Wang** – Tianjin Institute of Environmental and Operational Medicine, Tianjin 300050, China; [orcid.org/0000-0003-1650-3297](https://orcid.org/0000-0003-1650-3297); Email: [wxxemail@sina.cn](mailto:wxxemail@sina.cn)

**Xiang-Yu Zhang** – School and Hospital of Stomatology, Tianjin Medical University, Tianjin 300070, China; [orcid.org/0000-0001-5350-5879](https://orcid.org/0000-0001-5350-5879); Email: [xzhang04@tmu.edu.cn](mailto:xzhang04@tmu.edu.cn)

### Authors

**Chong Feng** – School and Hospital of Stomatology, Tianjin Medical University, Tianjin 300070, China; Tianjin Institute of Environmental and Operational Medicine, Tianjin 300050, China

**Yan Liu** – Tianjin Institute of Environmental and Operational Medicine, Tianjin 300050, China; Lanzhou University, Lanzhou 730000, China

**Bao-Yi Zhang** – Tianjin Institute of Environmental and Operational Medicine, Tianjin 300050, China

**Hao Zhang** – School and Hospital of Stomatology, Tianjin Medical University, Tianjin 300070, China; Tianjin Institute of Environmental and Operational Medicine, Tianjin 300050, China

**Fa-Yu Shan** – School and Hospital of Stomatology, Tianjin Medical University, Tianjin 300070, China; Tianjin Institute of Environmental and Operational Medicine, Tianjin 300050, China

**Tian-Qi Li** – School and Hospital of Stomatology, Tianjin Medical University, Tianjin 300070, China; Tianjin Institute of Environmental and Operational Medicine, Tianjin 300050, China

**Zhi-Ning Zhao** – School and Hospital of Stomatology, Tianjin Medical University, Tianjin 300070, China

Complete contact information is available at:

<https://pubs.acs.org/10.1021/acsomega.3c01289>

### Author Contributions

X.-X.W. and X.-Y.Z. designed the project and critically revised the manuscript. C.F. designed and performed most experiments and wrote the draft. Y.L., B.-Y.Z., and H.Z. performed experiments. F.-Y.S., T.-Q.L., and Z.-N.Z. performed data curation, visualization, and software. All authors have read and agreed to the published version of the manuscript.

### Funding

This work was supported by grants from the National Natural Science Foundation of China (NSFC) (grant nos. 31971106, BWS211013, 21WS09002, and JK20211A010213).

### Notes

The authors declare no competing financial interest.

Compliance to ethical norms. All animal experiments were performed at the Tianjin Institute of Environmental and Operational Medicine. All animal procedures were carried out in accordance with the guidelines of the Experimental Animal Welfare and Ethics Committee of the Tianjin Institute of Environmental and Operational Medicine.

## ■ ACKNOWLEDGMENTS

We appreciate technical support from Amizona and HUABIO.

## ■ REFERENCES

- (1) Yu, W.; Zhong, L.; Yao, L.; Wei, Y.; Gui, T.; Li, Z.; Kim, H.; Holdreith, N.; Jiang, X.; Tong, W.; et al. Bone marrow adipogenic lineage precursors promote osteoclastogenesis in bone remodeling and pathologic bone loss. *J. Clin. Invest.* **2021**, *131*, No. e140214.
- (2) Boyle, W. J.; Simonet, W. S.; Lacey, D. L. Osteoclast differentiation and activation. *Nature* **2003**, *423*, 337–342.
- (3) Grill, V.; Martin, T. J. Metabolic bone diseases. *Med. J. Aust.* **1995**, *163*, 38–41.
- (4) Hu, Y.; Wang, Y.; Chen, T.; Hao, Z.; Cai, L.; Li, J. Exosome: Function and Application in Inflammatory Bone Diseases. *Oxid. Med. Cell. Longevity* **2021**, *2021*, 1–17.
- (5) Fan, Z.; Pathak, J.; Ge, L. The Potential Role of RP105 in Regulation of Inflammation and Osteoclastogenesis During Inflammatory Diseases. *Front. Cell Dev. Biol.* **2021**, *9*, 713254.
- (6) Suda, T.; Takahashi, N.; Udagawa, N.; Jimi, E.; Gillespie, M. T.; Martin, T. J. Modulation of osteoclast differentiation and function by the new members of the tumor necrosis factor receptor and ligand families. *Endocr. Rev.* **1999**, *20*, 345–357.
- (7) Luo, J.; Yang, Z.; Ma, Y.; Yue, Z.; Lin, H.; Qu, G.; Huang, J.; Dai, W.; Li, C.; Zheng, C.; et al. LGR4 is a receptor for RANKL and negatively regulates osteoclast differentiation and bone resorption. *Nat. Med.* **2016**, *22*, 539–546.
- (8) Glantschnig, H.; Fisher, J. E.; Wesolowski, G.; Rodan, G. A.; Reszka, A. A. M-CSF, TNF $\alpha$  and RANK ligand promote osteoclast survival by signaling through mTOR/S6 kinase. *Cell Death Differ.* **2003**, *10*, 1165–1177.

- (9) Jaber, F. A.; Khan, N. M.; Ansari, M. Y.; Al-Adlaan, A. A.; Hussein, N. J.; Safadi, F. F. Autophagy plays an essential role in bone homeostasis. *J. Cell. Physiol.* **2019**, *234*, 12105–12115.
- (10) Lee, N. K.; Choi, Y. G.; Baik, J. Y.; Han, S. Y.; Jeong, D. W.; Bae, Y. S.; Kim, N.; Lee, S. Y. A crucial role for reactive oxygen species in RANKL-induced osteoclast differentiation. *Blood* **2005**, *106*, 852–859.
- (11) He, X.; Andersson, G.; Lindgren, U.; Li, Y. Resveratrol prevents RANKL-induced osteoclast differentiation of murine osteoclast progenitor RAW 264.7 cells through inhibition of ROS production. *Biochem. Biophys. Res. Commun.* **2010**, *401*, 356–362.
- (12) Hong, G.; Chen, Z.; Han, X.; Zhou, L.; Pang, F.; Wu, R.; Shen, Y.; He, X.; Hong, Z.; Li, Z.; et al. A novel RANKL-targeted flavonoid glycoside prevents osteoporosis through inhibiting NFATc1 and reactive oxygen species. *Clin. Transl. Med.* **2021**, *11*, No. e392.
- (13) Zhou, J.; Yang, J.; Dong, Y.; Shi, Y.; Zhu, E.; Yuan, H.; Li, X.; Wang, B. Oncostatin M receptor regulates osteoblast differentiation via extracellular signal-regulated kinase/autophagy signaling. *Stem Cell Res. Ther.* **2022**, *13*, 278.
- (14) Tong, X.; Zhang, C.; Wang, D.; Song, R.; Ma, Y.; Cao, Y.; Zhao, H.; Bian, J.; Gu, J.; Liu, Z. Suppression of AMP-activated protein kinase reverses osteoprotegerin-induced inhibition of osteoclast differentiation by reducing autophagy. *Cell Proliferation* **2020**, *53*, No. e12714.
- (15) Xu, H.; Yu, Y.; Zheng, Q.; Zhang, W.; Wang, C. D.; Zhao, X. Y.; Tong, W. X.; Wang, H.; Liu, P.; Zhang, X. L. Autophagy protects end plate chondrocytes from intermittent cyclic mechanical tension induced calcification. *Bone* **2014**, *66*, 232–239.
- (16) Zhao, H.; Sun, Z.; Ma, Y.; Song, R.; Yuan, Y.; Bian, J.; Gu, J.; Liu, Z. Antiosteoclastic bone resorption activity of osteoprotegerin via enhanced AKT/mTOR/ULK1-mediated autophagic pathway. *J. Cell. Physiol.* **2020**, *235*, 3002–3012.
- (17) Zoncu, R.; Efeyan, A.; Sabatini, D. M. mTOR: from growth signal integration to cancer, diabetes and ageing. *Nat. Rev. Mol. Cell Biol.* **2011**, *12*, 21–35.
- (18) Efeyan, A.; Sabatini, D. M. mTOR and cancer: many loops in one pathway. *Curr. Opin. Cell Biol.* **2010**, *22*, 169–176.
- (19) Hosokawa, N.; Hara, T.; Kaizuka, T.; Miura, Y.; Iemura, S. i.; Kishi, C.; Takamura, A.; Natsume, T.; Takehana, K.; Yamada, N.; et al. Nutrient-dependent mTORC1 association with the ULK1-Atg13-FIP200 complex required for autophagy. *Mol. Biol. Cell* **2009**, *20*, 1981–1991.
- (20) Zhang, Y.; Xu, S.; Li, K.; Tan, K.; Liang, K.; Wang, J.; Shen, J.; Zou, W.; Hu, L.; Cai, D.; et al. mTORC1 Inhibits NF- $\kappa$ B/NFATc1 Signaling and Prevents Osteoclast Precursor Differentiation, In Vitro and In Mice. *J. Bone Miner. Res.* **2017**, *32*, 1829–1840.
- (21) Dai, Q.; Xie, F.; Han, Y.; Ma, X.; Zhou, S.; Jiang, L.; Zou, W.; Wang, J. Inactivation of Regulatory-associated Protein of mTOR (Raptor)/Mammalian Target of Rapamycin Complex 1 (mTORC1) Signaling in Osteoclasts Increases Bone Mass by Inhibiting Osteoclast Differentiation in Mice. *J. Biol. Chem.* **2017**, *292*, 196–204.
- (22) Lai, C.; Chen, Z.; Ding, Y.; Chen, Q.; Su, S.; Liu, H.; Ni, R.; Tang, Z. Rapamycin Attenuated Zinc-Induced Tau Phosphorylation and Oxidative Stress in Rats: Involvement of Dual mTOR/p70S6K and Nrf2/HO-1 Pathways. *Front. Immunol.* **2022**, *13*, 782434.
- (23) Eid, A. A.; Ford, B. M.; Bhandary, B.; de Cassia Cavagliero, R.; Block, K.; Barnes, J. L.; Gorin, Y.; Choudhury, G. G.; Abboud, H. E. Mammalian target of rapamycin regulates Nox4-mediated podocyte depletion in diabetic renal injury. *Diabetes* **2013**, *62*, 2935–2947.
- (24) Shan, M.; Qin, J.; Jin, F.; Han, X.; Guan, H.; Li, X.; Zhang, J.; Zhang, H.; Wang, Y. Autophagy suppresses isoprenaline-induced M2 macrophage polarization via the ROS/ERK and mTOR signaling pathway. *Free Radical Biol. Med.* **2017**, *110*, 432–443.
- (25) Fang, S.; Wan, X.; Zou, X.; Sun, S.; Hao, X.; Liang, C.; Zhang, Z.; Zhang, F.; Sun, B.; Li, H.; et al. Arsenic trioxide induces macrophage autophagy and atheroprotection by regulating ROS-dependent TFEB nuclear translocation and AKT/mTOR pathway. *Cell Death Dis.* **2021**, *12*, 88.
- (26) Sun, M.; Ji, Y.; Li, Z.; Chen, R.; Zhou, S.; Liu, C.; Du, M. Ginsenoside Rb3 Inhibits Pro-Inflammatory Cytokines via MAPK/AKT/NF- $\kappa$ B Pathways and Attenuates Rat Alveolar Bone Resorption in Response to Porphyromonas gingivalis LPS. *Molecules* **2020**, *25*, 4815.
- (27) An, J. Y.; Kerns, K. A.; Ouellette, A.; Robinson, L.; Morris, H. D.; Kaczorowski, C.; Park, S. I.; Mekvanich, T.; Kang, A.; McLean, J. S.; et al. Rapamycin rejuvenates oral health in aging mice. *Elife* **2020**, *9*, No. e54318.
- (28) Lin, H.; Yan, J.; Wang, Z.; Hua, F.; Yu, J.; Sun, W.; Li, K.; Liu, H.; Yang, H.; Lv, Q.; et al. Loss of immunity-supported senescence enhances susceptibility to hepatocellular carcinogenesis and progression in Toll-like receptor 2-deficient mice. *Hepatology* **2013**, *57*, 171–182.
- (29) Niu, Y. B.; Yang, Y. Y.; Xiao, X.; Sun, Y.; Zhou, Y. M.; Zhang, Y. H.; Dong, D.; Li, C. R.; Wu, X. L.; Li, Y. H.; et al. Quercetin prevents bone loss in hindlimb suspension mice via stanniocalcin 1-mediated inhibition of osteoclastogenesis. *Acta Pharmacol. Sin.* **2020**, *41*, 1476–1486.
- (30) Lee, S.; Kim, H. S.; Kim, M. J.; Min, K. Y.; Choi, W. S.; You, J. S. Glutamine metabolite  $\alpha$ -ketoglutarate acts as an epigenetic cofactor to interfere with osteoclast differentiation. *Bone* **2021**, *145*, 115836.
- (31) Mohamad Hazir, N. S.; Yahaya, N. H. M.; Zawawi, M. S. F.; Damanhuri, H. A.; Mohamed, N.; Alias, E. Changes in Metabolism and Mitochondrial Bioenergetics during Polyethylene-Induced Osteoclastogenesis. *Int. J. Mol. Sci.* **2022**, *23*, 8331.
- (32) Rajput, S. A.; Shaukat, A.; Wu, K.; Rajput, I. R.; Baloch, D. M.; Akhtar, R. W.; Raza, M. A.; Najda, A.; Rafał, P.; Albrakati, A.; et al. Luteolin Alleviates AflatoxinB1-Induced Apoptosis and Oxidative Stress in the Liver of Mice through Activation of Nrf2 Signaling Pathway. *Antioxidants* **2021**, *10*, 1268.
- (33) Huynh, H.; Wan, Y. mTORC1 impedes osteoclast differentiation via calcineurin and NFATc1. *Commun. Biol.* **2018**, *1*, 29.
- (34) Cai, Z. Y.; Yang, B.; Shi, Y. X.; Zhang, W. L.; Liu, F.; Zhao, W.; Yang, M. W. High glucose downregulates the effects of autophagy on osteoclastogenesis via the AMPK/mTOR/ULK1 pathway. *Biochem. Biophys. Res. Commun.* **2018**, *503*, 428–435.
- (35) Filomeni, G.; De Zio, D.; Cecconi, F. Oxidative stress and autophagy: the clash between damage and metabolic needs. *Cell Death Differ.* **2015**, *22*, 377–388.
- (36) Zhang, W.; Feng, C.; Jiang, H. Novel target for treating Alzheimer's Diseases: Crosstalk between the Nrf2 pathway and autophagy. *Ageing Res. Rev.* **2021**, *65*, 101207.
- (37) Avenaggiato, M.; Vernucci, E.; Barreca, F.; Russo, M. A.; Tafani, M. Sirtuins' control of autophagy and mitophagy in cancer. *Pharmacol. Ther.* **2021**, *221*, 107748.
- (38) Rodríguez-Vargas, J. M.; Ruiz-Magaña, M. J.; Ruiz-Ruiz, C.; Majuelos-Melguizo, J.; Peralta-Leal, A.; Rodríguez, M. I.; Muñoz-Gómez, J. A.; de Almodóvar, M. R.; Siles, E.; Rivas, A. L.; Rivas, A. L.; et al. ROS-induced DNA damage and PARP-1 are required for optimal induction of starvation-induced autophagy. *Cell Res.* **2012**, *22*, 1181–1198.
- (39) Stern, M.; McNew, J. A. A transition to degeneration triggered by oxidative stress in degenerative disorders. *Mol. Psychiatry* **2021**, *26*, 736–746.
- (40) Zhang, Y.; Zhang, J.; Wang, S. The Role of Rapamycin in Healthspan Extension via the Delay of Organ Aging. *Ageing Res. Rev.* **2021**, *70*, 101376.
- (41) Adamopoulos, I. E.; Mellins, E. D. Alternative pathways of osteoclastogenesis in inflammatory arthritis. *Nat. Rev. Rheumatol.* **2015**, *11*, 189–194.
- (42) Mbalaviele, G.; Novack, D. V.; Schett, G.; Teitelbaum, S. L. Inflammatory osteolysis: a conspiracy against bone. *J. Clin. Invest.* **2017**, *127*, 2030–2039.
- (43) Rad, R.; Dossumbekova, A.; Neu, B.; Lang, R.; Bauer, S.; Saur, D.; Gerhard, M.; Prinz, C. Cytokine gene polymorphisms influence mucosal cytokine expression, gastric inflammation, and host specific

colonisation during *Helicobacter pylori* infection. *Gut* **2004**, *53*, 1082–1089.

(44) Neurath, M. F.; Finotto, S. IL-6 signaling in autoimmunity, chronic inflammation and inflammation-associated cancer. *Cytokine Growth Factor Rev.* **2011**, *22*, 83–89.

(45) Indran, I. R.; Liang, R. L.; Min, T. E.; Yong, E. L. Preclinical studies and clinical evaluation of compounds from the genus *Epimedium* for osteoporosis and bone health. *Pharmacol. Ther.* **2016**, *162*, 188–205.

(46) Wei, L.; Chen, W.; Huang, L.; Wang, H.; Su, Y.; Liang, J.; Lian, H.; Xu, J.; Zhao, J.; Liu, Q. Alpinetin ameliorates bone loss in LPS-induced inflammation osteolysis via ROS mediated P38/PI3K signaling pathway. *Pharmacol. Res.* **2022**, *184*, 106400.

(47) Xian, Y.; Su, Y.; Liang, J.; Long, F.; Feng, X.; Xiao, Y.; Lian, H.; Xu, J.; Zhao, J.; Liu, Q.; et al. Oroxylin A reduces osteoclast formation and bone resorption via suppressing RANKL-induced ROS and NFATc1 activation. *Biochem. Pharmacol.* **2021**, *193*, 114761.

(48) Shao, S.; Fu, F.; Wang, Z.; Song, F.; Li, C.; Wu, Z. X.; Ding, J.; Li, K.; Xiao, Y.; Su, Y.; et al. Diosmetin inhibits osteoclast formation and differentiation and prevents LPS-induced osteolysis in mice. *J. Cell. Physiol.* **2019**, *234*, 12701–12713.

(49) Kahan, B. D.; Gibbons, S.; Tejpal, N.; Stepkowski, S. M.; Chou, T. C.; Chou, T. C. Synergistic interactions of cyclosporine and rapamycin to inhibit immune performances of normal human peripheral blood lymphocytes in vitro. *Transplantation* **1991**, *51*, 232–238.

(50) Gerada, C.; Ryan, K. M. Autophagy, the innate immune response and cancer. *Mol. Oncol.* **2020**, *14*, 1913–1929.